

Novel Continuous Terminal Sliding Mode Observer Based Sensorless Speed Control of PMSM Drive System

Abdul Khaliq Junejo¹, Mohsin Ali Koondhar^{1,*}, Rizwan Aziz Siddiqui¹, Ghulam Sarwar Kaloi¹, Muhammad Ali Bijarani¹

Abstract:

The permanent magnet synchronous motor (PMSM) control is a demanding task because, which is a nonlinear multivariable coupling system. The vector control has been widely used in the control of PMSM system, where the rotor position information is needed for close loop control system. The mechanical sensors are used for rotor position, which increased the cost of the system. These sensors can be eliminated by adopting the sensor less control methods. In this paper a new continuous terminal sliding mode observer (CTSMO) based speed sensor less control method is proposed, which is substitute of the conventional SMO (CSMO). The suggested CTSMO is robust against parametric change and load disturbances, which is used to estimate the speed and rotor position from the back EMF (BEMF) of the PMSM system. The conventional SMO needs the low pass filter (LPF), position compensation techniques and sigmoid function instead of sign function to decrease the chattering phenomena. To eliminate the chattering phenomena effectively the new CTSMO based speed sensor less method is designed in this paper, which has also ability of minimization of the speed and rotor position error. The stability of the proposed technique is analyzed by Lyapunov function, the simulation have been carried out for the validation of the suggested technique.

Keywords: *PMSM, sliding mode control (SMC), conventional SMO (CSMO), continuous terminal sliding mode observer*

¹ Department of Electrical Engineering, Quaid-e-Awam University of Engineering Science and Technology, Nawabshah, 67450, Pakistan

1. Introduction

Chattering phenomena refer to rapid, repeated oscillations or fluctuations that occur in dynamic systems, particularly when there are discontinuities or switching behaviors[1]. This phenomenon is often observed in control systems, mechanical systems, and electrical systems, where the system rapidly alternates between different states due to instability or undesirable interactions[2]. The significant research is being conducting to estimate rotor position or speed sensor less drives for PMSMs that have equal dynamic effect to sensor based drives systems[3, 4]. The PMSM drives have been widely applicable from servo to traction drives because of many distinguishing characteristics for instance better controllability, large torque, high power density, high efficiency to ruggedness and inertia ratio [5-8]. The use of PMSM drive system in commercial has recently increased dramatically. The Field oriented control is widely adopted in PMSM drive system, which a precise rotor needs position for smooth control.

The resolvers and encoders are generally used to provide an accurate rotor position for close loop system. However, in some harsh environments, these devices are costly and unreliable and these encoders and resolvers need extra installation space. As a result, sensor less control is gaining popularity in recent research. The sensor less approaches are classified into two types: one is based on machine modeling [9-12] and another is mathematical model. Anisotropy-based methods are appropriate for sensor less operation at low and zero speeds [13-15]. The rotor position of machine can be determined by injecting high frequency signals (IHFS) into it. Though, IHFS would increase in torque ripple and power losses[16]. The techniques based on mathematical model are appropriate for sensor less control for medium and high speeds. The speed rotor and position can be predictable back EMF (BEMF), which is regarded as a standard sensor less control solution in the industrial sector. When machine anisotropy based approaches are

combined with machine model based techniques. Then, the wind range sensor less operation would be possible[17].

However, the estimated BEMF has high current ripple, which is the inherent problem of conventional, the estimators. Therefore, it is recommended to propose a suitable sensor less control method, which has small current ripple. The sliding mode based observer (SMO) are used many time inside a single current control (SCC) cycle to lessen the additional inaccuracy in calculating the BEMF in the current control loop (CCL) [18]. Additional rotor and a LPF position compensation are employed in a traditional SMO to mitigate the chattering problem frequently encountered in SMOs apply a signum function. As a switching function, the SMO currently employs a sigmoid function. The observer responds quickly and has robustness built into the design parameters [19]. The chattering can be decreased by employing the signum function (SF) in SMO [20]. The Stability of the SMO is checked thorough Lypunov function. The stator resistance must be determined because it

$$\begin{aligned} \frac{d\hat{i}_\alpha}{dt} &= \frac{1}{L} \{-R\hat{i}_\alpha + \mu_\alpha - k\text{sign}(\hat{i}_\alpha - i_\alpha)\} \\ \frac{d\hat{i}_\beta}{dt} &= \frac{1}{L} \{-R\hat{i}_\beta + \mu_\beta - k\text{sign}(\hat{i}_\beta - i_\beta)\} \end{aligned} \quad (3)$$

changes when motor runs [18, 19]. One CTSMO is suggested to make sensor less control method robust beside load disturbance and parameter fluctuations. The CTSMO estimates the BEMF in a current control cycle, which eliminates the current ripples. As a result, a quick and precise estimation of the BEMF based CTSMO is obtained with small chattering in the rotor velocity estimation.

2. Mathematical Modeling of PMSM Drive Systems

PMSM sensor less control is dependent on the BEMF estimation. Hence, the PMSM model must be in stationary frame. The PMSM stator comprises of 3Ø windings, which are positioned in the stator and

displaced 120° apart in the circle [21]. These three phases can be reduced to a fixed axis often known as a two-phase model (stationary-frame). The stator voltage state variable equations in stationary frame are written as

$$\frac{di_\alpha}{dt} = \frac{1}{L} \{-Ri_\alpha - \varepsilon_\alpha + \mu_\alpha\} \quad (1)$$

$$\begin{aligned} \frac{di_\beta}{dt} &= \frac{1}{L} \{-Ri_\beta - \varepsilon_\beta + \mu_\beta\} \\ \varepsilon_\alpha &= \lambda\omega_r \sin(\theta_e) \\ \varepsilon_\beta &= \lambda\omega_r \cos(\theta_e) \end{aligned} \quad (2)$$

Where i_α and i_β are the actual current of α and β - axis, μ_α and μ_β are the actual voltage of α and β - axis. ε_α and ε_β are the BEMF of the PMSM and R, L and λ are the parameters of stator resistance, inductance and BEMF constant, θ_e and ω_r are the position and speed of the rotor [22].

2.1. Conventional SMO (CSMO)

The SMC has the advantage of restricting the states variables on the designed sliding trajectory, which also changes with structure change [23]. The SMC is a well-known control approach that is commonly used in non-linear control systems due to its robustness against the load disturbances and parametric variation[24]. In terms of SMO, the SMC can be employed for sensor less approaches. However, there are some drawbacks to the SMO, such as chattering and time delay [25]. The two phase stationary axis

of PMSM drive system for the conventional SMO can be stated as [26].

Where i_α and i_β are the actual currents, \hat{i}_α and \hat{i}_β are the estimated currents of α and β - axis and k is the constant gain of the SMO. The stator equations with the error of the stationary axis currents can be rewritten as [27].

$$\begin{aligned} \frac{d\hat{i}_\alpha}{dt} &= \frac{1}{L} \{-R\hat{i}_\alpha + \mu_\alpha - k\text{sign}(\bar{i}_\alpha)\} \\ \frac{d\hat{i}_\beta}{dt} &= \frac{1}{L} \{-R\hat{i}_\beta + \mu_\beta - k\text{sign}(\bar{i}_\beta)\} \end{aligned} \quad (4)$$

$$\text{Where } [\bar{i}_\alpha \bar{i}_\beta]^T = [\hat{i}_\alpha - i_\alpha \hat{i}_\beta - i_\beta]^T \mathbf{I}$$

In accordance with structure theory of sliding mode variable (SMV), the system states will reach on sliding trajectory, when $k > \max(|\varepsilon_\alpha|, |\varepsilon_\beta|)$. Therefore, the BEMF obtained as

$$\begin{aligned} \varepsilon_\alpha &= k\text{sign}(\bar{i}_\alpha) \\ \varepsilon_\beta &= k\text{sign}(\bar{i}_\beta) \end{aligned} \quad (5)$$

The BEMF equations (5) can be used to approximation speed and position of PMSM drive system. The sign function is employed for the traditional SMO technique, which causes the significant chattering in the system states. Since, high switching gains are needed to approximate the BEMF for speed and position of PMSM drive system [28]. As a result, the LPF is adopted to eliminate chattering from the system states, which is depicted in the Fig. 1.

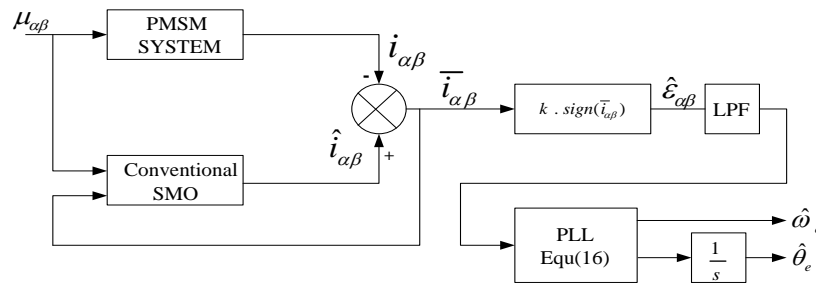


Fig. 1. Conventional SMO diagram

Therefore, it is required that to present a novel SMO to reduce aforementioned problems and minimizing the speed and rotor errors, respectively [29]. The CTSMO is

suggested in this paper, which can solve the aforementioned problems from the drive systems effectively.

2.2. CTSMO Design

The SMV structure has been classified into reaching and sliding phase, for the reaching phase a control law is required and for sliding phase a sliding mode surface is needed. Therefore, the CTSMO is chosen as SMO to estimate the BEMFs. The CTSMO can reduce the chattering phenomena effectively from the system state and improve the convergence rate, tracking precision than that of the conventional SMO, which can be written as [30].

$$\sigma = \dot{\bar{i}}_{\sigma} + k|\bar{i}_{\sigma}|^{\delta} \text{sign}(\bar{i}_{\sigma}) \quad (6)$$

Where,

The p and q are the odd positive numbers, and $1 < \frac{p}{q} < 2$. The reaching law is playing a key part in the SMO, and it may be stated as [31].

$$\dot{\alpha} = k_1 \text{sign}(\sigma) \quad (7)$$

According to the design of control Law, the \bar{i}_{σ} and i_{α}^* can converge to zero in the finite time, when sliding mode surface converge to zero as $\bar{i}_{\sigma} = i_{\sigma}^* = 0$. The equation (3) rewritten as

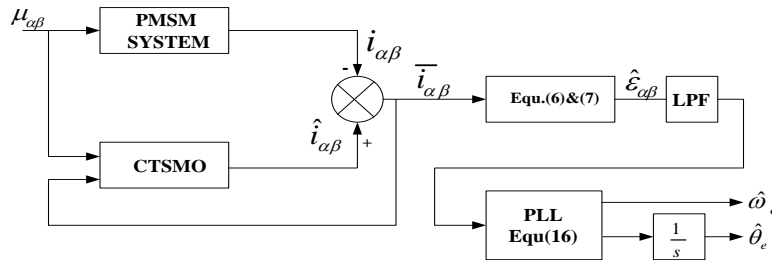


Fig. 2. Proposed CTSMO

2.2.1. Stability Analysis

$$\frac{di}{dt} = \frac{1}{L}(-R\bar{i} + \varepsilon + \chi) \quad (8)$$

Where, $\bar{i} = [\bar{i}_{\alpha} \ \bar{i}_{\beta}]^T$, $\varepsilon = [\varepsilon_{\alpha} \ \varepsilon_{\beta}]^T$ and $\chi = [\chi_{\alpha} \ \chi_{\beta}]^T$ are the vector estimated error current, vector back EMF and vector input control respectively.

Theorem 1. The final control law of based on CTSMO (10) can be designed from (7) and (8). In the final control law there are two terms one is equivalent control law (χ_{eq}), which is based on machines parameters and another is switching law χ_{sw} , which based on CTSMO. In a finite amount of time, the system's state would converge to zero.

$$\chi = \chi_{eq} + \chi_{sw} \quad (10)$$

$$\chi_{eq} = R\bar{i} \quad (11)$$

$$\chi_{sw} = -\int_0^t L \frac{p}{q} k |i_{\sigma}|^{\frac{p}{q}-1} + k_1 \text{sign}(\sigma) dt \quad (12)$$

Therefore, the estimated BEMF based on the CTSMO are described as

$$\hat{\varepsilon} = -(\hat{i}^{\&} + k|\bar{i}| \text{sign}(\bar{i})) - \int k_1 \text{sign}(\bar{i}) dt \quad (13)$$

Where, $\hat{\varepsilon} = [\hat{\varepsilon}_{\alpha} \ \hat{\varepsilon}_{\beta}]^T$ and $\hat{i}^{\&} = [\hat{i}_{\alpha}^{\&} \ \hat{i}_{\beta}^{\&}]^T$ and proposed CTSMO diagram for PMSM drive system is depicted in Fig. 2.

To verify permanence of the suggested observer, the Lyapunov function has been selected, which can be described as[32].

$$V = 1/2\sigma^T \sigma \quad (14)$$

The stability according to Lyapunov function is expressed as

$$\begin{aligned} \dot{V} &= \sigma^T \dot{\sigma} \\ \dot{V} &= S^T \left[i_\sigma + \frac{p}{q} k \text{diag} \left(i_\sigma \right)^{\frac{p-1}{q}} i_\sigma \right] \\ &= \frac{p}{q} k \text{diag} \left(i_\sigma \right)^{\frac{p-1}{q}} \left[i_\sigma + k^{-1} \frac{q}{p} i_\sigma^{\frac{2-p}{q}} \right] \end{aligned}$$

From equations 7 to 10, the i_σ written as

$$\begin{aligned} i_\sigma &= (\varepsilon + x_{SW}) / L \\ \dot{V} &= \frac{p}{q} k \text{diag} \left(i_\sigma \right)^{\frac{p-1}{q}} \left[(\varepsilon + x_{sw}) / L + k^{-1} \frac{q}{p} i_\sigma^{\frac{2-p}{q}} \right] \\ &= \frac{1}{L} \frac{p}{q} k \text{diag} \left(i_\sigma \right)^{\frac{p-1}{q}} \left[(\varepsilon + x_{sw}) + k^{-1} \frac{p}{q} i_\sigma^{\frac{2-p}{q}} - k_1 \text{sign}(\sigma) \right] \\ \dot{V} &\leq -\frac{1}{L} \frac{p}{q} k \text{diag} \left(i_\sigma \right)^{\frac{p-1}{q}} \left[k_1 \text{sign}(\sigma) \right] \leq 0 \end{aligned}$$

Since, the p and q are the odd positive numbers, which can be describe as

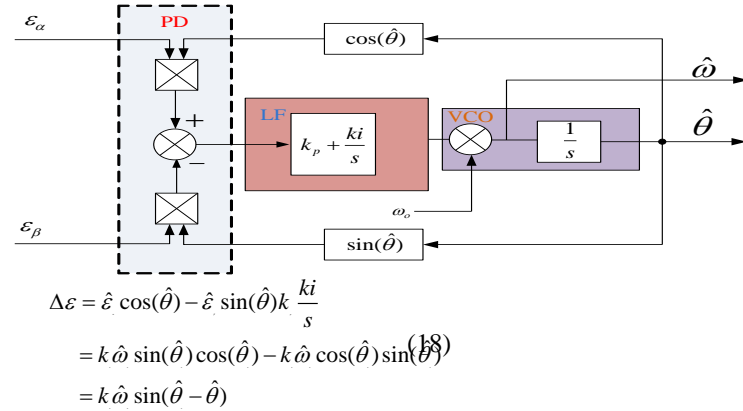
$$1 < p/q < 2, \text{ if } i_n^{\frac{p-1}{q}} = 0 \text{ when } i_n \neq 0. \text{ If } i_n^{\frac{p-1}{q}} = 0 \text{ when } i_n = 0.$$

Fig. 3. Equivalent diagram of PLL

Where $\hat{\omega}_e$ and $\hat{\theta}_e$ are the predictable position and speed of rotor, which are associated with back EMF, $\hat{\theta}$ is the rotor position which is predictable by PLL. When

3. Design of Phase Locked Loop (PLL) For Speed Estimation

From (9), the estimated $\varepsilon = [\varepsilon_\alpha \varepsilon_\beta]^T$ are



used to approximate the speed and position $\hat{\omega}_e$ and $\hat{\theta}_e$ by applying the arc-tan function.

$$\hat{\theta}_e = \arctan(\hat{\varepsilon}_\alpha / \hat{\varepsilon}_\beta) \quad (16)$$

$$\hat{\omega}_e = \frac{d}{dt}(\hat{\theta}_e) \quad (17)$$

The main limitation of the conventional SMO is chattering, which is produced by the switching function and the derivation of the position produced the chopping in the speed of the system. These limitations can be solved by using CTSMO and PLL respectively.

The PLL has the significant advantages over the frequency and phase is illustrated in Fig. 3, which can be obtained from equation (17) and described as in equation 18.

$\hat{\theta}_e - \hat{\theta} < \frac{\pi}{6}$, then the approximation taken as $\sin(\hat{\theta}_e - \hat{\theta}) \approx \hat{\theta}_e - \hat{\theta}$ Fig. 4 illustrates the PPL diagram.

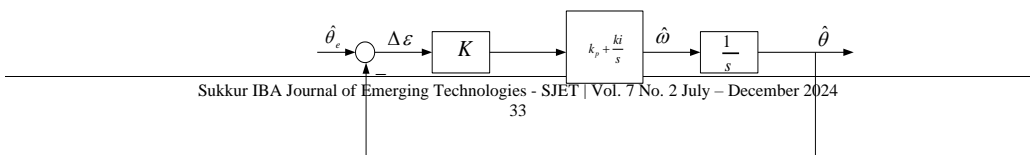


Fig. 4. PLL Equivalent Block diagram

By utilizing the PLL approach, the proposed senseless control method can improve industrial applications. The regulator can directly determine the speed from the angle error, and the integrator can estimate the rotor position [33]. The input signal of PLL can the estimated from BEMF, and the position signal can be derived from the BEMF, respectively. The PLL's bandwidth is determined by the rated speed, motor inertia, speed and current controllers. The bandwidth of the PLL must be within the mid band of speed and current controllers for the nonsensical technique to work. According to the literature, the band width of a PLL is often varied from 10-20 times the speed loop bandwidth, ensuring faultless tracking. The bandwidth of the PLL is based on the k_p and k_i gains, the transfer function closed loop of PLL can be described as [34].

$$H(s) = \frac{k s + k}{s + k s + k} \quad (19)$$

Where the operating factor and damping frequencies expressed as

$$\xi = \frac{k_p}{2\sqrt{k_i}}, \quad \omega_n = \sqrt{k_i} \quad (20)$$

4. Results and Discussions

To verify the suggested control scheme a model is developed in the MATLAB. Parameters of simulation for the proposed PLL-based CTSMO method for sensorless PMSM control are illustrated in Table 1.

TABLE I. Parameters of the PMSM

Factors	Quantity and unit
Supply phases	3
Machine pole pairs	3
Rated Power	3.0 kW
Armature Resistance	0.8Ω
Rotor flux linkage	0.35 wb
Stator induction	0.005 H
Moment of inertia	$3.78 \times 10^{-4} kg.m^2$
Viscous density	$1.74 \times 10^{-5} Nms/rad$

To check the robustness of the suggested

technique, the drive performance is assessed in dynamic condition under the speeds of 1000 rpm, which are illustrated in Figs. 5 and 6, respectively.

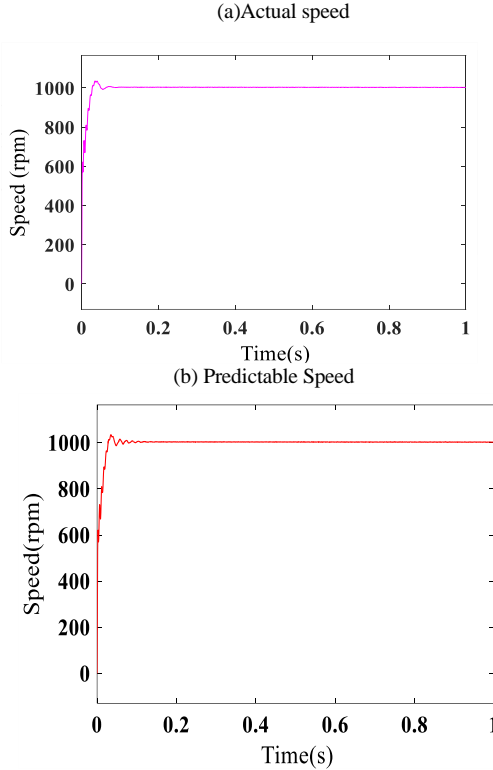
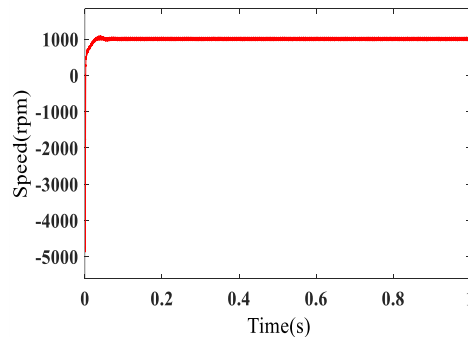
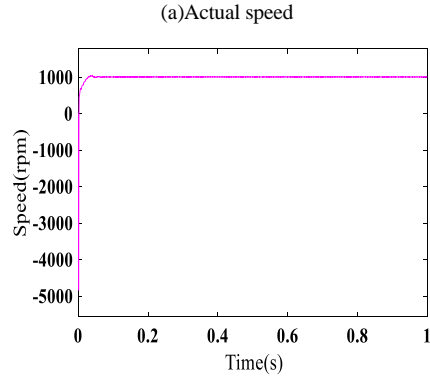


Fig. 5. PMSM's dynamic speed response under the CSMO simulation





(a)Actual speed

(b) Predictable Speed

Fig. 6. CTSMO-simulated dynamic speed response of the PMSM

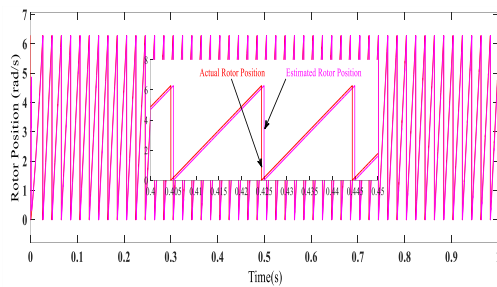


Fig. 7. Simulated dynamic rotor position ($\hat{\theta}$) response and actual of the PMSM under the CSMO

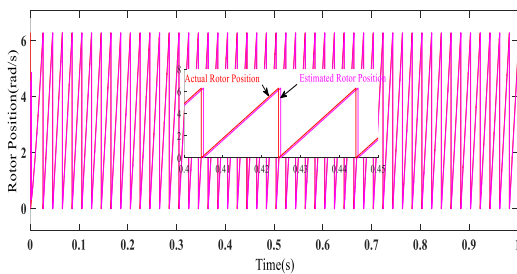


Fig. 8. Simulated dynamic rotor position ($\hat{\theta}$) response and actual of the PMSM under the CTSMO

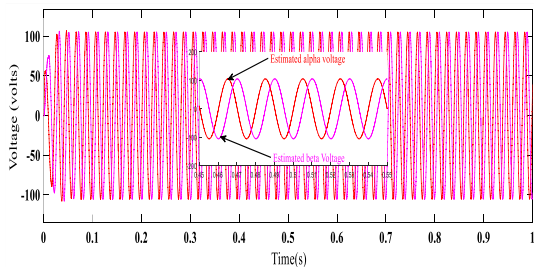


Fig. 9. Simulated dynamic estimated alpha-beta $X_{\alpha\beta}$ response of the PMSM under the CSMO

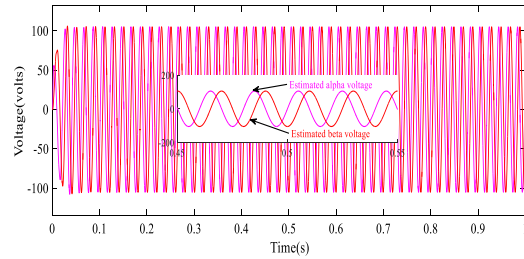


Fig. 10. Simulated dynamic estimated alpha-beta ($X_{\alpha\beta}$) response of the PMSM under the CTSMO

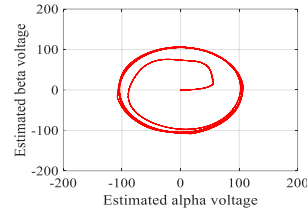


Fig. 11. Simulated circular axis alpha-beta ($X_{\alpha\beta}$) response of the PMSM under the CSMO

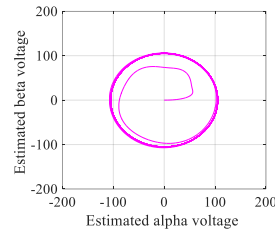


Fig. 12. Simulated circular axis alpha-beta ($X_{\alpha\beta}$) response of the PMSM under the CTSMO.

It can be easily seen in the same picture that the speed deviation smaller with proposed method than of the conventional technique. Moreover, the predictable and actual rotor positions are evaluated under proposed method and conventional method, which are shown in Fig. 7 and 8, separately. It is observable that the predictable error in the position signal under proposed technique is very small than that of conventional technique. It is observable that the predictable error in the position signal under proposed technique is very small than that of

conventional technique as shown in Figures 9, 10, 11, 12.

Furthermore, it can be observed from Figs. 14, 15, and 16 that the estimated alpha-beta ($X_{\alpha\beta}$) voltage response, estimated alpha-beta ($i_{\alpha\beta}$) current response and estimated speed error response of the PMSM under conventional and proposed method that the suggested technique has better response than the conventional method, respectively.

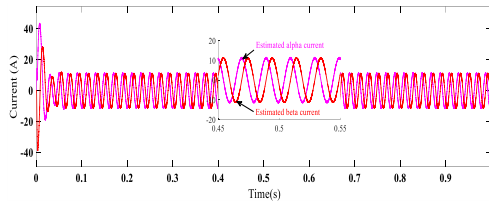


Fig. 13. Simulated dynamic estimated alpha-beta ($i_{\alpha\beta}$) response of the PMSM under the CSMO

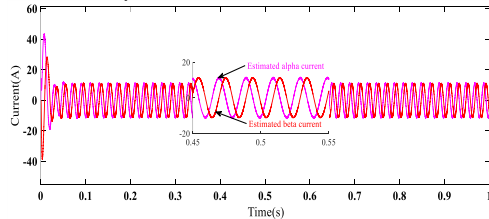
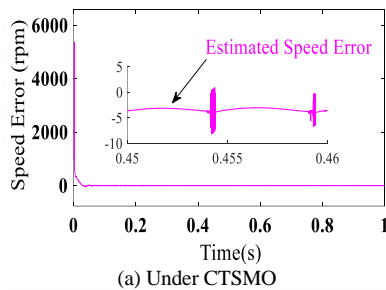
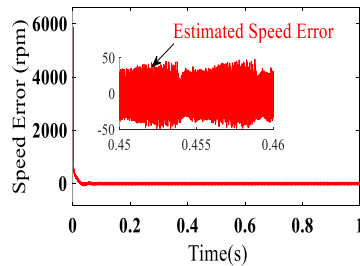


Fig. 14. Simulated dynamic estimated alpha-beta ($i_{\alpha\beta}$) response of the PMSM under the conventional SMO



(a) Under CTSMO



(b) Under conventional SMO

Fig. 15. Simulated dynamic estimated speed error response of the PMSM

5. Conclusion

In this paper, a novel continuous terminal sliding mode observer (CTSMO) technique has been developed and applied for sensor less speed control of permanent magnet synchronous motors (PMSMs) integrated with a phase-locked loop (PLL). The proposed CTSMO overcomes the traditional limitations of the conventional Sliding Mode Observer (SMO), particularly the issue of **chattering**, which is effectively minimized. Chattering, a well-known drawback of conventional SMOs, can lead to undesirable high-frequency oscillations and degraded system performance. By adopting the CTSMO, the system achieves smoother control dynamics, enhancing the overall operational reliability and robustness.

The results demonstrate that the proposed CTSMO offers superior performance in terms of speed error and position error compared to the conventional SMO. This improvement is attributed to the inherent characteristics of the CTSMO design, which ensures more accurate estimation and robust control, even under varying operating conditions.

To ensure the stability of the proposed approach, the Lyapunov stability criterion was employed. The use of the Lyapunov function validates that the system remains stable throughout its operation, providing theoretical support for the robustness and reliability of the CTSMO methodology.

The simulation results validate the advantages of the proposed sensor less speed control approach. The CTSMO outperforms the conventional SMO in critical performance metrics, including precision, stability, and the ability to handle system uncertainties. These results highlight the effectiveness and potential of the CTSMO as a viable

alternative for high-performance, sensor less PMSM speed control applications, paving the way for advancements in motor drive systems.

Abbreviations/ Nomenclature	
BEMF	Back EMF
CTSMO	Continuous Terminal Sliding Mode Observer
CSMO	Conventional Sliding Mode Observer
CCL	Current Control Loop
IHFS	Injecting High Frequency Signals
LPF	Low Pass Filter
PMSM	Permanent Magnet Synchronous Motor
PLL	Phase Locked Loop
SMO	Sliding Mode Observer
SCC	Single Current Control
SF	Signum Function

References

[1] A. Rehan, I. Boiko, and Y. Zweiri, "Chaotic Chattering in Sliding Mode Control Systems," IEEE Transactions on Automatic Control, 2024.

[2] P. De Rua, T. Roose, Ö. C. Sakinci, N. d. M. D. Campos, and J. Beerten, "Identification of mechanisms behind converter-related issues in power systems based on an overview of real-life events," Renewable and Sustainable Energy Reviews, vol. 183, p. 113431, 2023.

[3] Y. Zuo, C. Lai, and K. L. V. Iyer, "A review of sliding mode observer based sensorless control methods for PMSM drive," IEEE Transactions on Power Electronics, vol. 38, pp. 11352-11367, 2023.

[4] S. Wang, H. Wang, C. Tang, J. Li, D. Liang, and Y. Qu, "Research on Control Strategy of Permanent Magnet Synchronous Motor Based on Fast Terminal Super-Twisting Sliding Mode Observer," IEEE Access, 2024.

[5] O. C. Kivanc and S. B. Ozturk, "Sensorless PMSM drive based on stator feedforward voltage estimation improved with MRAS multiparameter estimation," IEEE/ASME Transactions on Mechatronics, vol. 23, pp. 1326-1337, 2018.

[6] F. Aghili, "Energy-efficient and fault-tolerant control of multiphase nonsinusoidal pm synchronous machines," IEEE/ASME Transactions on Mechatronics, vol. 20, pp. 2736-2751, 2015.

[7] T. D. Do, H. H. Choi, and J.-W. Jung, "Nonlinear optimal DTC design and stability analysis for interior permanent magnet synchronous motor drives," IEEE/ASME Transactions on Mechatronics, vol. 20, pp. 2716-2725, 2015.

[8] X. Zhang and G. H. B. Foo, "A constant switching frequency-based direct torque control method for interior permanent-magnet synchronous motor drives," IEEE/ASME Transactions on Mechatronics, vol. 21, pp. 1445-1456, 2015.

[9] D. Liang, J. Li, and R. Qu, "Sensorless control of permanent magnet synchronous machine based on second-order sliding-mode observer with online resistance estimation," IEEE Transactions on Industry Applications, vol. 53, pp. 3672-3682, 2017.

[10] G. Wang, L. Yang, G. Zhang, X. Zhang, and D. Xu, "Comparative investigation of pseudorandom high-frequency signal injection schemes for sensorless IPMSM drives," IEEE

- Transactions on Power Electronics, vol. 32, pp. 2123-2132, 2016.
- [11] D. Kim, Y.-C. Kwon, S.-K. Sul, J.-H. Kim, and R.-S. Yu, "Suppression of injection voltage disturbance for high-frequency square-wave injection sensorless drive with regulation of induced high-frequency current ripple," *IEEE Transactions on Industry Applications*, vol. 52, pp. 302-312, 2015.
- [12] P. Xu and Z. Zhu, "Novel carrier signal injection method using zero-sequence voltage for sensorless control of PMSM drives," *IEEE Transactions on Industrial Electronics*, vol. 63, pp. 2053-2061, 2015.
- [13] M. M. Ismail, W. Xu, J. Ge, Y. Tang, A. K. Junejo, and M. G. Hussien, "Adaptive linear predictive model of an improved predictive control of permanent magnet synchronous motor over different speed regions," *IEEE Transactions on Power Electronics*, vol. 37, pp. 15338-15355, 2022.
- [14] W. Xu, A. K. Junejo, Y. Tang, M. Shahab, H. U. R. Habib, Y. Liu, et al., "Composite speed control of PMSM drive system based on finite time sliding mode observer," *IEEE Access*, vol. 9, pp. 151803-151813, 2021.
- [15] W. Xu, A. K. Junejo, Y. Liu, M. G. Hussien, and J. Zhu, "An efficient antidisturbance sliding-mode speed control method for PMSM drive systems," *IEEE Transactions on Power Electronics*, vol. 36, pp. 6879-6891, 2020.
- [16] L. Chen, H. Zhang, H. Wang, K. Shao, G. Wang, and A. Yazdani, "Continuous adaptive fast terminal sliding mode-based speed regulation control of pmsm drive via improved super-twisting observer," *IEEE Transactions on Industrial Electronics*, vol. 71, pp. 5105-5115, 2023.
- [17] X. Wei, K. Mei, S. Ding, and L. Jiang, "Sensorless control of permanent magnet synchronous motor based on fixed-time terminal sliding mode observer," *Asian Journal of Control*, vol. 26, pp. 1771-1786, 2024.
- [18] H. Lee and J. Lee, "Design of iterative sliding mode observer for sensorless PMSM control," *IEEE Transactions on Control Systems Technology*, vol. 21, pp. 1394-1399, 2012.
- [19] H. Kim, J. Son, and J. Lee, "A high-speed sliding-mode observer for the sensorless speed control of a PMSM," *IEEE transactions on Industrial Electronics*, vol. 58, pp. 4069-4077, 2010.
- [20] Y. Mousavi, G. Bevan, I. B. Kucukdemiral, and A. Fekih, "Sliding mode control of wind energy conversion systems: Trends and applications," *Renewable and Sustainable Energy Reviews*, vol. 167, p. 112734, 2022.
- [21] R. Krishnan, T. Isha, and P. Balakrishnan, "A back-EMF based sensorless speed control of permanent magnet synchronous machine," in *2017 International Conference on Circuit, Power and Computing Technologies (ICCPCT)*, 2017, pp. 1-5.
- [22] Z. Qiao, T. Shi, Y. Wang, Y. Yan, C. Xia, and X. He, "New sliding-mode observer for position sensorless control of permanent-magnet synchronous motor," *IEEE Transactions on Industrial electronics*, vol. 60, pp. 710-719, 2012.
- [23] L. Song, J. Huang, Q. Liang, L. Nie, X. Liang, and J. Zhu, "Trajectory Tracking Strategy for Sliding Mode Control with Double Closed-Loop

- for Lawn Mowing Robot Based on ESO," *IEEE Access*, 2022.
- [24] L. Yu, J. Huang, W. Luo, S. Chang, H. Sun, and H. Tian, "Sliding-Mode Control for PMLSM Position Control—A Review," in *Actuators*, 2023, p. 31.
- [25] X. Zou, H. Ding, and J. Li, "Sensorless Control Strategy of Permanent Magnet Synchronous Motor Based on Fuzzy Sliding Mode Controller and Fuzzy Sliding Mode Observer," *Journal of Electrical Engineering & Technology*, pp. 1-15, 2022.
- [26] E. Lu, W. Li, X. Yang, and Y. Liu, "Anti-disturbance speed control of low-speed high-torque PMSM based on second-order non-singular terminal sliding mode load observer," *ISA transactions*, vol. 88, pp. 142-152, 2019.
- [27] S. Liu, Q. Wang, G. Wang, B. Li, D. Ding, G. Zhang, et al., "Virtual-Axis Injection Based Online Parameter Identification of PMSM Considering Cross Coupling and Saturation Effects," *IEEE Transactions on Power Electronics*, 2023.
- [28] L. Li, W. Zhou, X. Bi, and X. Shi, "Speed Estimation of PMSM Based on a Super-Twisting Slide Mode Observer," *Machines*, vol. 10, p. 681, 2022.
- [29] F. Gao, Z. Yin, C. Bai, D. Yuan, and J. Liu, "A Lag Compensation-Enhanced Adaptive Quasi-Fading Kalman Filter for Sensorless Control of Synchronous Reluctance Motor," *IEEE Transactions on Power Electronics*, vol. 37, pp. 15322-15337, 2022.
- [30] L. Mo, Y. Liu, and Y. Zhang, "Sliding mode variable structure control for surface permanent magnet synchronous motors based on a fuzzy exponential reaching law," *Mathematical Problems in Engineering*, vol. 2019, 2019.
- [31] Z. Yin, Y. Zhang, X. Tong, and Y. Zhong, "Model predictive control using globe exponential reaching law sliding mode design method for induction motor drives," in *2019 IEEE Applied Power Electronics Conference and Exposition (APEC)*, 2019, pp. 2559-2563.
- [32] E. Zhao, J. Yu, J. Liu, and Y. Ma, "Neuroadaptive dynamic surface control for induction motors stochastic system based on reduced-order observer," *ISA transactions*, vol. 128, pp. 318-328, 2022.
- [33] C. Gu, X. Wang, X. Shi, and Z. Deng, "A PLL-based novel commutation correction strategy for a high-speed brushless DC motor sensorless drive system," *IEEE Transactions on Industrial Electronics*, vol. 65, pp. 3752-3762, 2017.
- [34] A. Nair, S. Kamalasan, J. Geis-Schroer, S. Patel, and M. Smith, "An Investigation of Grid Stability and a New Design of Adaptive Phase-Locked Loop for Wind-Integrated Weak Power Grid," *IEEE Transactions on Industry Applications*, vol. 58, pp. 5871-5884, 2022.